# Understanding The Dynamics Of Vapor Intrusion Processes

Brown University

Jonathan G. V. Ström

Spring 2020

# Contents

# Chapter 1

# Preferential Pathways: Drivers Of Temporal And Spatial Variability In Vapor Intrusion

**Abstract**

Preferential pathways have recently been recognized for the significant role that they may play in enhancing vapor intrusion (VI). The nature and specific effect of a preferential pathway can vary greatly and is largely site specific; generalizing their impact can therefore be difficult. Two well-studied VI sites were revealed to be characterized by preferential pathways, providing an excellent opportunity to explore their influence. One of these sites was in Layton, Utah, which featured a preferential pathway that had a very significant impact on, among other things, but in particular, the temporal variability of indoor contaminant concentration. This preferential pathway was at a later date closed, and the comparison between the periods before and after the closing offers some unprecedented opportunities for understanding preferential pathways. A preferential pathway similar to that one will be implemented in our numerical model, and through analysis of data from the site, will offer insights how preferential pathways can enhance VI. The implications of these insights have wider consequences for VI investigations in general, which is further explored in Chapter (TBD). Another well-studied site in Indianapolis, Indiana, was also affected by a preferential pathway, but its role and influence was very different from the Layton site, and in particular played a significant role in the spatial variability of subsurface contaminant concentrations, a topic which will explored using data from the site, as well as from the Layton site.

## 1.1 Introduction

Long term vapor intrusion (VI) studies in both residential and larger commercial structures have raised concerns regarding significant observed transient behavior in indoor air contaminant concentrations[1, 2, 3, 4, 5, 6, 7], a phenomena that has previously been observed at houses impacted by radon intrusion[8]. Such variations make it difficult for those charged with protecting human health to formulate a response and appropriate risk evaluation. Furthermore there is uncertainty within the VI community regarding how to best develop sampling strategies to address this problem[1, 3, 9, 6].

To address these concerns, the EPA purchased two VI impacted houses and outfitted them with a wide variety of sensors and sampling instrumentation to study VI at these houses in great detail. Indoor contaminant concentration as well soil-gas and groundwater contaminant concentration at different depths and locations were recorded, while simultaneously recording metrics such as indoor and outdoor temperature, wind speed and direction, and building pressurization. These measurements were taken continuously over multiple years an unprecedented detailed dataset for exploring VI.

One of these houses was in Layton, Utah, near Hill AFB, and was purchased in collaboration with a research group at Arizona State University (ASU), who conducted most of the research at the site - this site will be referred to as the "ASU house" throughout this work[3]. The other was in duplex in Indianapolis, Indiana, and will be referred to as the "EPA duplex". There work was not primarily isolated to one group.

One thing both of these sites had in common was that after a few years of study, preferential pathways were discovered at the sites. A preferential pathway is typically thought of as some conduit that can transport large amounts of contaminant vapors into a building, in contrast with the slower vapor transport in soils.

At the ASU house, this took the form of a land drain underneath the house foundation, presumably to drain excess water from the sub-slab region. This land drain was connected to the nearby sewer and exited into a gravel layer under the foundation, near a breach in the slab. The sewer was buried deep enough to be partially submerged in the TCE contaminated groundwater, which likely infiltrated into the sewer. The land drain was later excavated and fitted with a valve, allowing the researchers to control its influence - which was revealed to be very significant[10]. The details of this is covered further down.

At the EPA duplex, the sewer acted as a preferential pathway, somewhat similar to the ASU house, but the nature of this preferential pathway was quite different from the one at the ASU house. A tracer gas test demonstrated that contaminant vapors were directly transported into the duplex[11]; similar to a site in Boston, Massachusetts, where PCE was transported into a bathroom through broken plumbing fixtures[12]. It was also demonstrated that contaminated groundwater infiltrated the sewer a few blocks away from the duplex, where a dry-cleaners had previously been. This type of distributed contamination via a sewer network has likewise been recorded in Denmark[13] as a VI source - giving rise to a very different situation compared to radon intrusion.

It is also likely that the sewer pipe at the duplex leaked contaminant vapors somewhere near the vicinity of the house. This would give a situation that is similar

to the ASU house land drain, but somewhat mitigated since the pipe leakiness is likely due to structural degradation, e.g. cracks in the mantle area; quite different from open channel flow from the ASU house land drain.

These works shows some of the diverse ways that a preferential pathway can play a role in VI (Figure 1.1 shows a visual summary of these ways), and our poor understanding in evaluating their significance. However, since the influence of the preferential pathway at the ASU house was able to be turned on and off (via the valve), we have an unprecedented opportunity to explore the effects of such a preferential pathway at a VI site.

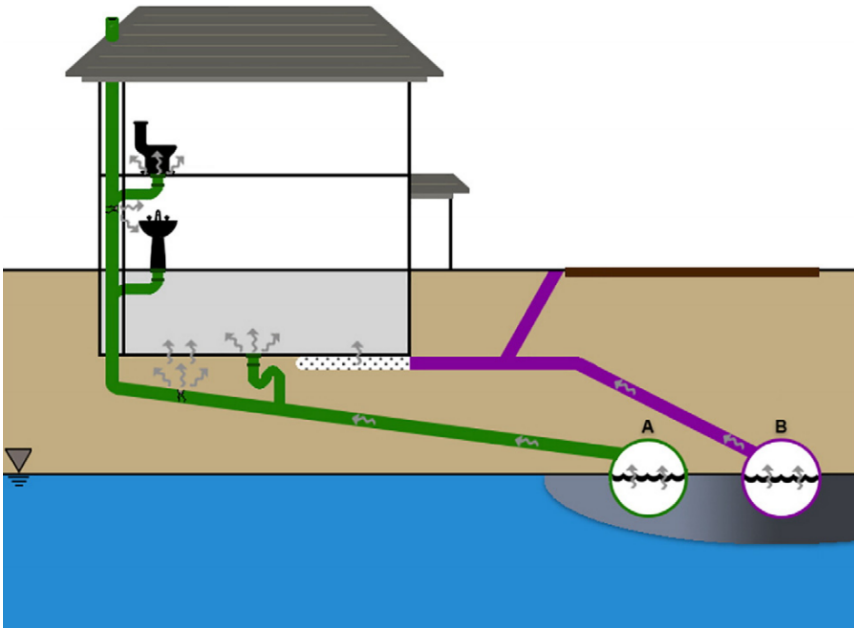


Figure 1.1: Visual summary of some of the different ways that contaminant infiltration, and ultimate transport into a VI affected building. Figure from McHugh et al.[11].

### 1.1.1 The ASU House

The VI study at the ASU house had primarily two purposes:

1. Investigate VI with a particular focus on understanding the temporal and spatial variability.

2. Test and evaluate the performance of the controlled pressure method (CPM).

This was to be achieved by monitoring various metrics relevant to VI, such as building pressurization, air exchange rate, indoor and outdoor temperature, and other metrological variables, while simultaneously monitoring the indoor air contaminant concentration. Additionally, soil-gas and groundwater contaminant concentration underneath and around the house were monitored; the specific sampling locations, as well as a photo of the house, can be seen in Figure 1.2a. The study of the ASU house is one of the most detailed studies of a VI site to date and fully describing the experimental setup and measured metrics is beyond the scope of this work but is detailed in Holton et al.[3].

(a) Picture of the "ASU house" from Holton et al.[3]

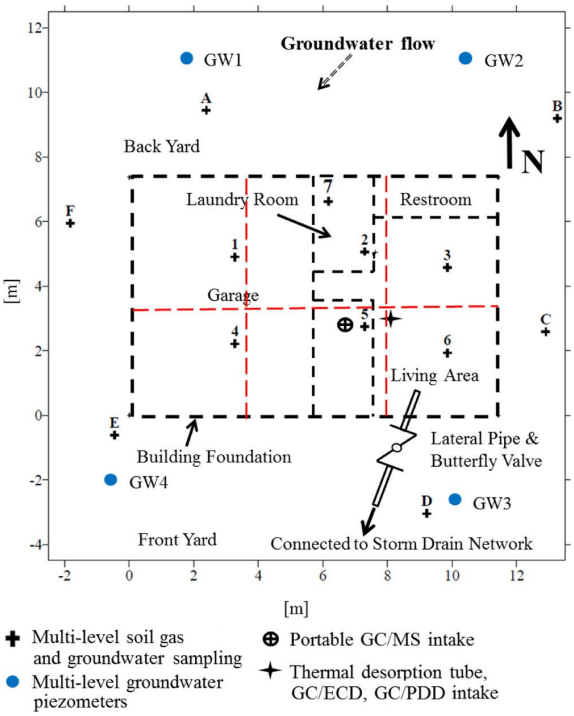


(b) Floor plan of the "ASU house". Locations of all sampling ports and of the land drain preferential pathway marked. Figure from Guo et al.[10].

CPM seeks to control the pressurization of the building, and thereby controlling the contaminant entry rate. In this framework, overpressurizing a building will eliminate contaminant entry rate into the building, thereby identifying indoor contaminant sources. By contrast, depressurizing a building will increase contaminant entry rate, giving a theoretical "worst-case" VI scenario. Here the researchers would use a 20 inch window box fan to control the pressurization of the building.

The site was monitored for roughly 1.5 years before the testing of the CPM system commenced. During this time, it was established that the indoor contaminant concentration fluctuated significantly at the site - roughly an order of magnitude on a weekly basis, while up to three or more orders of magnitude on a seasonal basis. Once the house was depressurized using the CPM system, indoor contaminant concentration increased to higher concentration levels previously recorded - an initial verification of the CPM framework[14].

However, during the CPM testing period, the researchers noticed that the house and nearby sewer seemingly communicated with each other. This was shown by the movement of a plastic tarp, which covered a nearby manhole, as the door of the house was opened and closed. This lead to the discovery of the land drain preferential pathway at the site; the location of it in relation to the house floorplan can be seen in Figure 1.2b The land drain determined to exit into the gravel sublayer beneath the foundation, near a visible breach in the foundation slab, and was subsequently excavated and fitted with a butterfly valve [10] to control its influence.

The land drain was closed towards the later part of the CPM study, which lead to a significant decrease in indoor contaminant concentration. This effect can be seen in Figure 1.3a, which shows the log-10 transformed indoor contaminant concentration

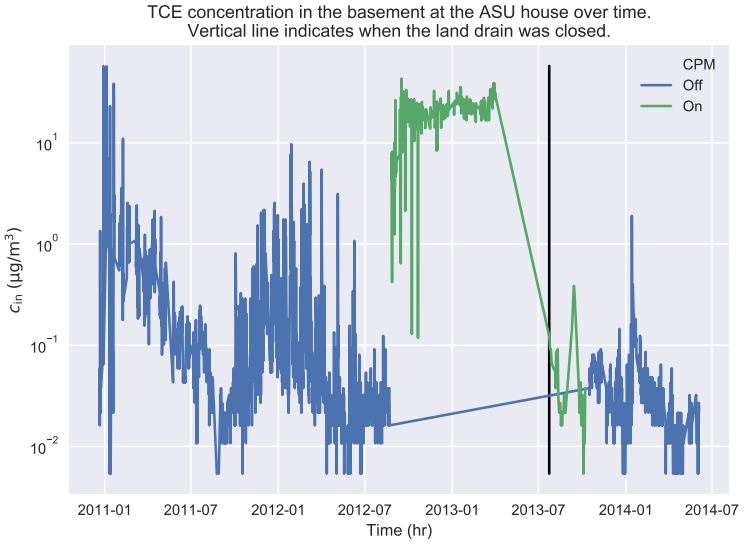


(a) The temporal variability of indoor air contaminant concentrations recorded at the ASU house. Measurements were taken in the basement. The periods were the CPM system was on and off are marked.

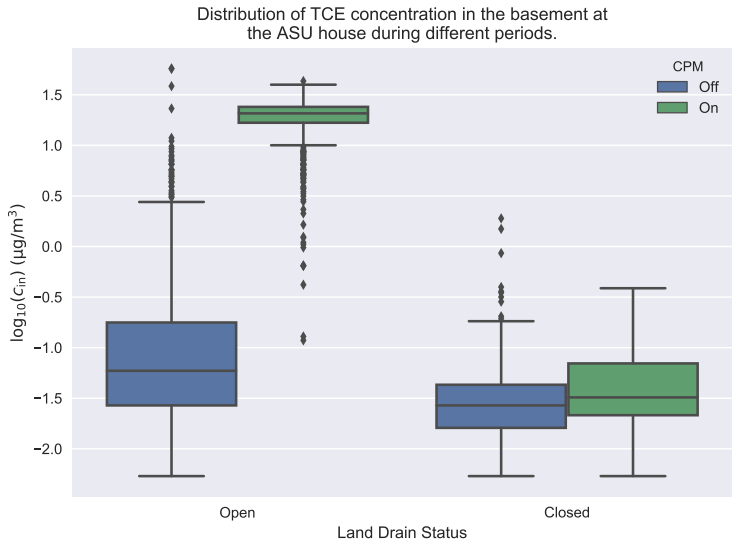


1

(b) Boxplot showing the log-10 transformed TCE concentrations at the ASU house. The CPM and natural periods, and the period before and after the land drain was closed are considered separately. The box signifies the interquartile range (IQR) of values, with the central line representing the median value, and the top and bottom of the box are the 25th and 75th percentiles. The whiskers extend to 1.5 times the IQR. Markers indicate outlier data points that fall outside the whiskers.

Figure 1.3

for the entire study duration. Here the pre- and post-CPM periods are marked by colors, and the closing of the land drain by the black vertical line. Notice how the temporal variability in indoor contaminant concentration decrease significantly after the closing of the land drain.

Figure 1.3b shows the same data, i.e. the log-10 transformed indoor contaminant concentration, but as a boxplot instead of a timeseries plot. Here the colored box

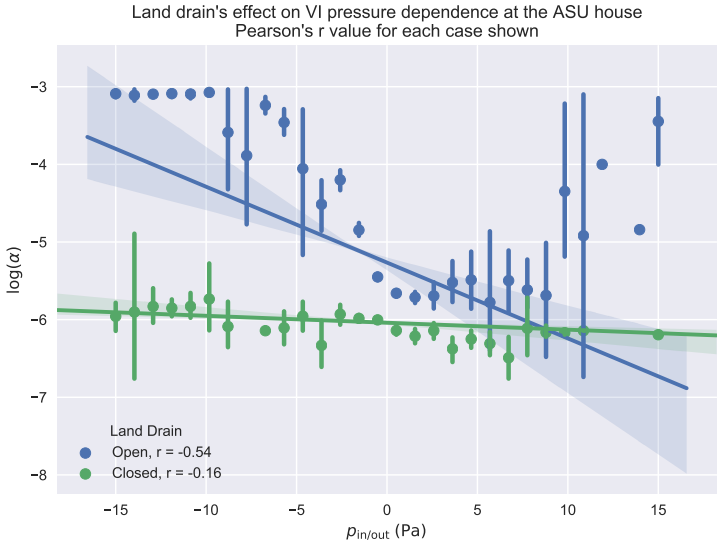


Figure 1.4: Regression plot showing the indoor/outdoor pressure difference dependence on indoor air concentration. Here the indoor air concentration is normalized to the groundwater source concentration, i.e. attenuation factor, and log-10 transformed. Data is placed in evenly spaced (but not sized) bins. The bars indicate the 95% confidence intervals.

represents the interquartile range (IQR) of the distribution - the middle line is the 50th or median value, while the top and bottom of the represent the 75th and 25th percentile values. The whiskers are the extent of the dataset, while "outlier" points are given by the dots, here formally defined as data lying 1.5 times outside the IQR; these are "real" data points but simply plotted as outliers not to skew the IQR. This figure again reinforces the significant effect that the land drain preferential pathway had on the temporal indoor contaminant concentration variability at the ASU house.

In the VI field, it is widely held that the building pressurization relative to the ambient outdoor is a key driver of contaminant entry into VI impacted building. Since building pressurization fluctuations can occurs rapidly, this is a prime factor for investigating the transport dynamics of the preferential pathway. Figure 1.4 considers the relationship between the indoor air concentration and building pressurization, specifically indoor/outdoor pressure difference, for the periods when the preferential pathway was open and closed. This clearly shows the dramatic change in sensitivity of the indoor contaminant concentration to building pressurization after the closing of the preferential pathway, which is not only apparent from visual inspect but from the change in the Pearson's r values for the considered periods. Pearson's r essentially tells us how linear correlation between two datasets; a value of 1 indicates that there is a perfect positive linear relationship, and -1 a perfectly negative linear relation. In our context, a negative value indicate that a decrease in building pressurization leads to an increase in indoor contaminant concentration, which makes sense as contaminant entry rates into the house would increase as it is further depressurized.

The question then becomes why this fundamental shift in the relationship between building pressurization and indoor contaminant concentration occurred, and

how it relates to temporal variability in indoor contaminant concentration. Answering this is one of the primary objectives of this chapter, which will be done by developing a numerical model of a VI site that is *similar* to the ASU house, and in combination with comparison to the field data, will give insights how a preferential pathway can fundamentally alters contaminant transport at a VI site. We will also explore how such a preferential pathway can significantly contribute to the spatial variability contaminant concentration, in particular in the near sub-surface region.

### 1.1.2 EPA Duplex

The EPA duplex was, similarly to the ASU house, a highly detailed VI study; Figure 1.5a shows a photo of the site. Here the indoor contaminant concentrations of TCE, PCE, chloroform, and radon were measured in different floors of each side of the duplex, as well as in different locations and depths in the subsurface and groundwater - these sampling location ports, as well as a floorplan of the duplex can be seen in Figure 1.5b. These sampling ports also allowed pressure differences between different locations to be measured. Metrological data was collected throughout the study period, which lasted for around 2.5 years, and included indoor and outdoor temperatures, wind speed and direction, precipitation, and recorded snow coverage[7]. The data from this site is publicly available online[15].

(a) Photo of the EPA duplex.

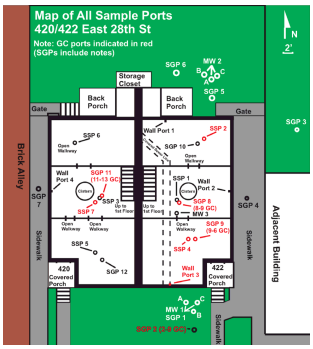


(b) Birdseye view of the EPA duplex, listing all the sampling location ports.

Figure 1.5

The was likewise characterized by significant temporal variability in indoor contaminant concentrations, which can be seen in Figure 1.6. This variability was not as significant as was recorded at the ASU house, but substantial nonetheless. Understanding the observed variability was a major focus of this study, but additionally the researchers sought to evaluate the efficacy of a subslab depressurization (SSD) system. A SSD system depressurizes the subslab region, which diverts contaminant vapors from entering the structure into a pipe placed through the foundation slab, which then are expelled into the atmosphere[7]. There are many different possible configurations of these pipes, and their design is its own research topic, one which will not be addressed in this work. However, it is useful to know, and we will only consider data before the implementation of the SSD system. It should also be noted that only one side of the duplex was heated, and we will only consider data from this side.

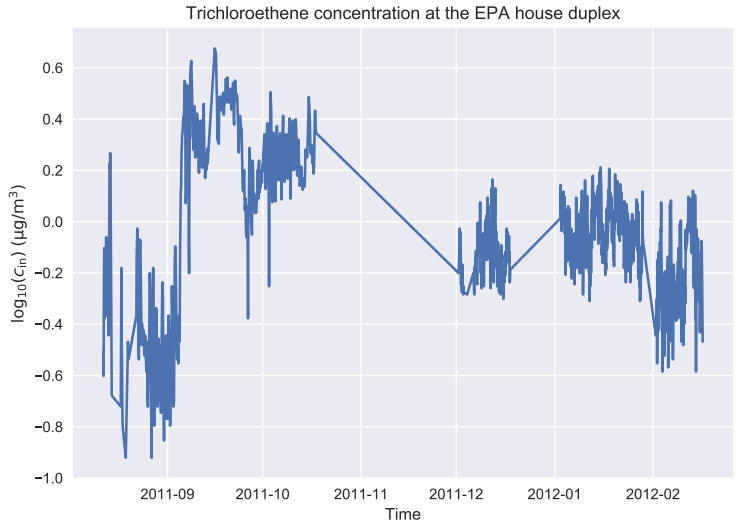


(a) Time series plot of the indoor TCE concentration in the heated side of the EPA duplex. Only the period before the SSD system was turned on considered.

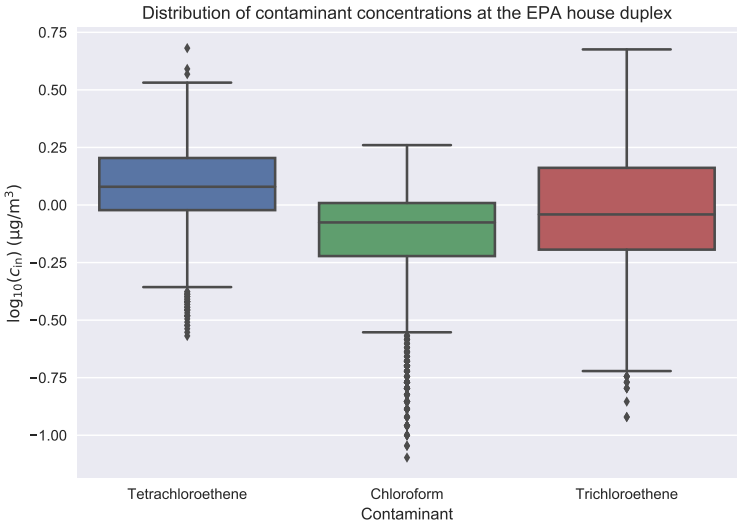


(b) Boxplot showing the distribution of log-10 transformed indoor concentration of three different contaminants in the heated side of the EPA duplex. The box is the interquartile range, with the line in the middle representing the median, and the top and bottom of the box representing the 75th and 25th percentiles respectively. The whiskers denote the extent of the data, with the points classified as "outliers", and are defined to be 1.5 times the IQR range.

Figure 1.6

Like the ASU house, it was later determined that a sewer preferential pathway existed at the site. This preferential pathway seemingly played a very different role than the one found at the ASU house, and different in primarily two ways:

1. Infiltration of contaminant vapors did not occur near the duplex, but instead occurred a few blocks away - at the site of an old dry cleaner.

2. Communication between this preferential pathway and the indoor environment does not seem to have been as strong; the researchers believe that this may be due to the poor condition of the sewer pipe, which may have leaked somewhere along its path.

The first of these points was demonstrated by McHugh et al.[11], which tracked contaminant vapors along the length of the sewer system. The second point, or rather the evidence that communication between the indoor environment and the preferential pathway may not have been so strong is indicated by the lower temporal indoor contaminant concentration variability. It is also indicated by the weaker association between indoor contaminant concentration and the indoor/outdoor pressure difference, which can be seen in Figure 1.7; this weaker association is indicated by the smaller Pearson's r values compared to the ones at the ASU house before he closing of that preferential pathway.

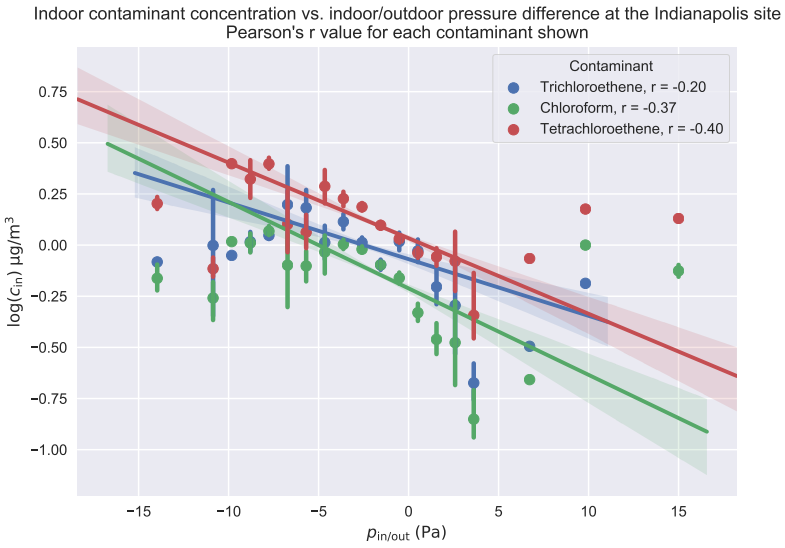


Figure 1.7: Relationship between indoor/outdoor pressure difference and indoor contaminant concentration of three contaminants - TCE, PCE, and chloroform at the EPA duplex.

Unfortunately, the EPA duplex preferential pathway is less well characterized, and its influence was never removed. This makes it difficult to assess how it contributed to overall VI at the site, or the observed temporal variability in indoor contaminant concentrations. However, it is possible to explore if the preferential pathway leaked somewhere near the site - which likewise will be a focus in this chapter.

Determining leakiness of the preferential pathway will be done by performing a kriging analysis of the measured soil-gas contaminant concentrations. Kriging is a type of interpolation technique which allows sparse data to be interpolated in multiple dimensions; ideal for interpolating soil-gas contaminant concentration in the soil surrounding the duplex. This way we can visually inspect the interpolated soil-gas contaminant concentration for "hot spots", which could indicate where such a leak might be.

## 1.2 Modeling A Preferential Pathway

To investigate the role a land drain type preferential pathway may have on a VI site, we extend the VI model presented in Chapter **??**. By adding a gravel sub-base layer underneath the foundation slab and a preferential pathway to this model, we develop a VI model scenario that is similar to the ASU house.

Here we assume the gravel sub-base layer is 30 cm thick and extends from the edges of the foundation slab. While the exact thickness of the gravel sub-base layer at the ASU house is not known, it was estimated to be roughly that thick. The soil surrounding the house is assumed to be homogenous sandy clay. This is based on a description of the soil, and was chosen as the most appropriate choice is some modeling work by Guo[16], one of the researchers at the ASU house.

The gravel sub-base, unlike the rest of the soil, is going to be relatively dry; it is covered by the foundation slab, so no rain infiltration will occur and due to the coarseness of the gravel, no moisture will be drawn up by capillary force. Nonetheless, some van Genuchten parameters for the gravel are necessary to solve the model. Additionally, based on the site description, we will assume that the surrounding soil is sandy clay, a , one of the researchers at the ASU house. Table **??** has the van Genuchten parameters used to model these.

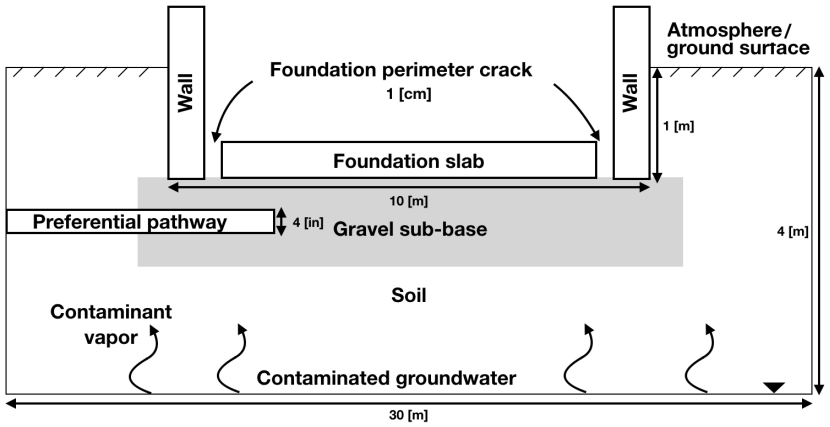


Figure 1.8: The modeled preferential pathway VI scenario.

Based on the description of the land drain preferential pathway at the ASU site, we will model a preferential pathway as 10 cm diameter pipe that exits at the interface between the soil and gravel sub-base layer; placing it near the foundation crack - similar to the ASU house[10]. Figure 1.8 shows the described scenario.

### 1.2.1 Geometry And Mesh

Explicitly modeling the entire preferential pathway in detail would requires a significant number of elements and at little gain; contaminant vapor transport in the far corners of the model are not of great interest. To save computational resources only the exit of the pipe is modeled as a 10 cm diameter circle.

The existence of the preferential pathway pipe circle, only one plane of symmetry exists instead of two, and half of the model geometry has to be explicitly constructed instead of just a quarter like in Chapter **??**.

The meshing of the model follows the steps detailed in Chapter **??**, with the exception that a boundary layer mesh generated on the preferential pathway circle; a similar initial mesh is generated with subsequent adaptive mesh refinement. Figure 1.9 shows the resulting meshed geometry.

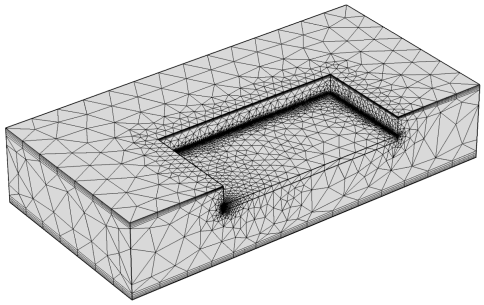

Figure 1.9: Meshed geometry of the preferential pathway model. Notice the gravel sub-base layer and the preferential pathway exit.

### 1.2.2 Physics And Boundary Conditions

In this model, we use the same governing equations introduced in Chapter **??**, but are included here for completeness. However, to simulate the preferential pathway, we will need to supply two new boundary conditions - one for the airflow in the soil governed by Darcy's Law, and another for the soil contaminant transport, which are discussed in their respective section below.

#### Indoor Environment

The indoor environment is modeled using:

$$V_{\text{bldg}}\frac{\partial c_{\text{in}}}{\partial t} = n_{\text{ck}} - V_{\text{bldg}}A_e c_{\text{in}}$$

$$n_{\text{ck}} = \int_{A_{\text{ck}}} j_{\text{ck}} dA$$

$$j_{ck} = \begin{cases} u_{ck}c_g - \frac{D_{\text{air}}}{L_{\text{slab}}}(c_{in} - c_g) & u_{ck} \geq 0 \\ u_{ck}c_{in} - \frac{D_{\text{air}}}{L_{\text{slab}}}(c_{in} - c_g) & u_{ck} < 0 \end{cases}$$

$c_{\text{in}}$ [mol m$^{-3}$] is the indoor contaminant concentration; $n_{\text{ck}}$ [mol s$^{-1}$] is the contaminant entry rate into the building via the foundation crack; $A_{\text{ck}}$ [m$^2$] is the foundation crack boundary area; $A_e = 0.5\,\text{h}^{-1}$ is the air exchange rate; $V_{\text{bldg}} = 300\,\text{m}^3$ is the volume of the house basement. $D_{\text{air}} = 7.2 \times 10^{-6}\,\text{m}^2\,\text{s}^{-1}$ is the diffusion coefficient of TCE in air; $u_{ck}$ [m s$^{-1}$] is the airflow velocity through the foundation crack; $L_{\text{slab}} = 15\,\text{cm}$ is the thickness of the foundation slab; and $c_g$ [mol m$^{-3}$] is the contaminant gas-phase concentration at the foundation crack boundary.

#### Soil Moisture

Soil moisture content is determined using van Genuchten's retention model. We use two "soil" types in this model - gravel and sandy clay; their parameters and

constants are shown in Table **??** in the appendix.

$$\mathrm{Se} = \begin{cases} \frac{1}{(1+(\alpha|h|)^n)^m} & h < 0 \\ 1 & h \geq 0 \end{cases}$$

$$\theta_w = \begin{cases} \theta_r + \mathrm{Se}(\theta_t - \theta_r) & h < 0 \\ \theta_t & h \geq 0 \end{cases}$$

$$k_r = \begin{cases} \mathrm{Se}^l \left[1 - \left(1 - \mathrm{Se}^{\frac{1}{m}}\right)\right]^2 & h < 0 \\ 0 & h \geq 0 \end{cases}$$

$$\theta_g = \theta_t - \theta_w$$

$h$ [m] is the elevation above the groundwater interface; Se is the saturation; $\alpha$, $m$, $n = \frac{1}{1-m}$, $l = 0.5$ are the van Genuchten parameters; $\theta_w$ is the water filled porosity; $\theta_g$ is the gas filled pororsity; $\theta_t$ is the soil porosity; $\theta_r$ is the residual moisture content. and $k_r$ is the relative permeability for water;

### Soil Airflow

Airflow is modeled using our modified Darcy's Law expression.

$$\frac{\partial}{\partial t}(\rho\theta_g) + \nabla \cdot \rho\Big( - \frac{(1-k_r)\kappa}{\mu}\nabla p\Big) = 0$$

$\vec{u}$ [$\mathrm{m\,s^{-1}}$] is the airflow velocity vector; $\kappa$ [$\mathrm{m^2}$] is the permeability of the porous medium; $\mu$ [$\mathrm{Pa\,s}$] is the dynamic viscosity of the fluid; $\nabla p$ [$\mathrm{Pa\,m^{-1}}$] is the pressure gradient; $\theta_g$ is the gas-filled porosity of the soil; $\rho = 1.225\,\mathrm{kg\,m^{-3}}$ is the density of air; and $\mu = 18.5 \times 10^{-6}\,\mathrm{Pa\,s}$ is the dynamic viscosity of air.

**Boundary conditions** Since the preferential pathway is assumed to be an open pipe, we assume it acts like a pressure gauge, just like the atmosphere, and is at the reference ambient atmospheric pressure.

| | |
|---|---|
| Ground surface | $p = 0\,\mathrm{Pa}$ |
| Preferential pathway | $p = 0\,\mathrm{Pa}$ |
| Foundation crack | $p = p_{\mathrm{in/out}}\,\mathrm{Pa}$ |
| Remaining | $-\vec{n} \cdot \rho\vec{u} = 0$ |

$p_{\mathrm{in/out}}$ is not specified here as we will parametrically choose values for it.

### Soil Contaminant Transport

The contaminant transport in the soil is governed by:

$$(\theta_w + \theta_g K_H)\frac{\partial c_w}{\partial t} = \nabla \cdot (D_{\mathrm{eff}}\nabla c_w) - K_H \vec{u}_g \cdot \nabla c_w$$

$c_w$ and $c_g$ [$\mathrm{mol\,m^{-3}}$] are the contaminant concentrations in water and gas respectively; $K_H = 0.402$ is the dimensionless Henry's Law constant for TCE at 20 °C; $\vec{u}_g$

$[\mathrm{m\,s^{-1}}]$ is the Darcy's velocity field; and $D_{\text{eff}}$ $[\mathrm{m^2\,s^{-1}}]$ is the effective diffusivity of the contaminant according to Millington-Quirks model:

$$D_{\text{eff}} = \left( D_w \frac{\theta_w^{\frac{10}{3}}}{\theta_t^2} + D_g \frac{\theta_g^{\frac{10}{3}}}{\theta_t^2} K_H \right)$$

$D_w = 1.02 \times 10^{-9}\,\mathrm{m^2\,s^{-1}}$ and $D_g = 6.87 \times 10^{-6}\,\mathrm{m^2\,s^{-1}}$ are the diffusion coefficient of TCE in water and air respectively;

**Boundary conditions** The air in the pipe is assumed to be contaminated with TCE at a vapor concentration equal to the vapor in equilibrium with the groundwater source contaminant concentration. This assumption is based on contaminant samples taken from a manhole near the ASU house[16] which demonstrated that contaminant vapor concentrations in the nearby sewer were on similar magnitude as near the contaminated groundwater source.

| | |
|---|---|
| Atmosphere | $c_w = 0\,\mathrm{mol\,m^{-3}}$ |
| Groundwater | $c_w = c_{gw}\ \mathrm{mol\,m^{-3}}$ |
| Preferential pathway | $c_g = c_{gw} K_H\ \mathrm{mol\,m^{-3}}$ |
| Foundation crack | $-\vec{n} \cdot \vec{N} = \dfrac{-j_{ck}}{K_H}\ \mathrm{mol\,m^{-2}\,s^{-1}}$ |
| All other | $-\vec{n} \cdot \vec{N} = 0\,\mathrm{mol\,m^{-2}\,s^{-1}}$ |

Note that we are neglecting any sorption in the soil, i.e. the sorption partitioning coefficient $K_p = 0\,\mathrm{m^3\,kg^{-1}}$. We will likewise normalize all concentrations to the source concentration $c_{gw}$, and any arbitrary value can be assigned.

## 1.3 Interpolating Soil-Gas Concentrations

*This is purposely left empty for now.*
contrasting

## 1.4 Temporal Variability And Preferential Pathways

In the calculation results shown in Figure 1.10, a preferential pathway is assumed to provide air containing contaminant vapor at a concentration equivalent to the vapor in equilibrium with the underlying groundwater source. Here, the indoor air exchange rate $A_e$ was assumed to be a constant 0.5 per hour, and $p_{\text{in/out}}$ was varied from -5 to 5 Pa. Values of predicted indoor air contaminant concentrations, $c_{\text{in}}$ were obtained from steady state calculations. The predicted $c_{\text{in}}$ values were then normalized by the assumed vapor concentration in equilibrium with groundwater $c_{\text{gw}}$, giving the attenuation from groundwater $\alpha_{\text{gw}}$. The predicted values of $\alpha_{\text{gw}}$ as a function of $p_{\text{in/out}}$ are given by the solid line Figure 1.10. These predicted values are compared to actual measured $\alpha_{\text{gw}}$ values from the ASU House for the period during which the preferential pathway was open given by the blue points.

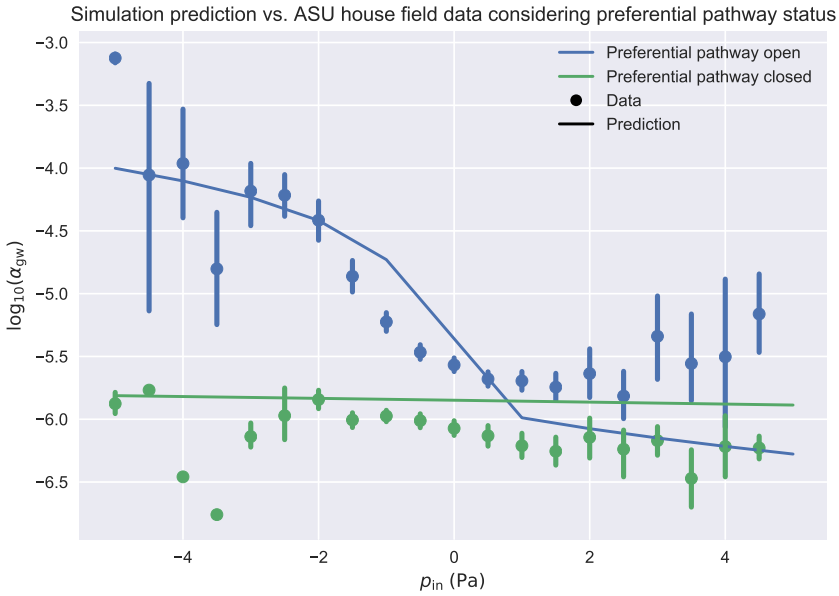


Figure 1.10: Model predicted indoor air concentration (as groundwater attenuation) compared to values recorded at the ASU house. The modeling results are given the solid lines and data by the dots. Blue here represents data before the closing of the preferential pathway and modeling result from the corresponding model, i.e. the model features a preferential pathway and a gravel sub-base. The green color signifies data from the period after the closing of the preferential pathway with the corresponding model, i.e. the preferential pathway is removed but the gravel sub-base remains. Here the data is placed in 20 equally *spaced bin*, i.e. not equally *sized*. The dot is the mean value and the error bars represent the 95% confidence intervals.

The model successfully predicts the observed trends in $\alpha_{gw}$ as $p_{in/out}$ decreases (increased depressurization) but somewhat underpredicts $\alpha_{gw}$ as the house is over-pressurized. Most significantly, the model captures that even for a small increase in depressurization (0 to -5 Pa) a very large increase in $\alpha_{gw}$ (two order of magnitude) can occur.

The model is also able to capture the weak trend in $\alpha_{gw}$ with $p_{in/out}$ when a preferential pathway is absent, but when there still exists a permeable subslab region. These results given by the green line in Figure 1.10. These results are again in agreement with what was observed at the ASU House when the preferential pathway was closed, i.e. that there was a much more modest variation in indoor air concentration, irrespective of pressure, when the preferential pathway was cut off.

This shows the significant contribution that such a preferential pathway may have at a VI site. First, the preferential pathway acts not only as a source of contaminant vapor, but also as a source of air to the subslab. Because of the large resistance to soil gas flow in the surrounding soil, having a local source of air to support the increase of advective flow into the structure from the subslab region makes a large difference.

While there obviously is still some variability unaccounted for, as indicated by the error bars in Figure 1.10, we can say with some confidence that the model is able to capture the general influence of such a preferential pathway. This opens us

up to explore some of the factors that may be crucial for such an influence. Using our model, we rerun some of the scenarios, but this time consider two more cases:

1. We remove the gravel sub-base layer but keep the preferential pathway.
2. We keep the gravel sub-base layer, but remove contaminant vapor from the preferential pathway, i.e. it contains "clean" air.

The results of running these cases can be seen in Figure 1.11.

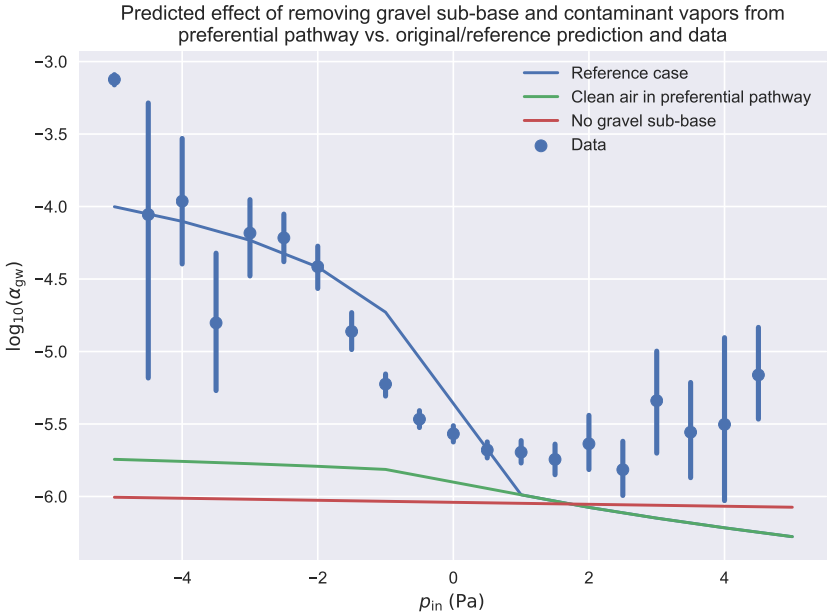


Figure 1.11: How different cases affect the predicted impact of the preferential pathway. The effect of removing the gravel sub-base, as well as a clean-air containing preferential pathway are considered.

Here the original modeling results and associated data from the period before the closing of the preferential pathway is again given by blue The case corresponding to the removal of contaminant vapors from the preferential pathway case is given by the green line, while the removal of the gravel sub-base care is given by red.

The removal of contaminant vapors from the preferential pathway largely eliminates the significant increase of $\alpha_{\text{gw}}$ with respect to $p_{\text{in}}$ as given by blue in Figure 1.10. However, the increase is larger than when the preferential pathway was absent as indicated by green in Figure 1.10. This shows that a preferential pathway similar to the one found at the ASU house does two things.

First, it provides a preferential source of air, and the depressurized building is able to much easier draw air from the preferential pathway than the surrounding soil; the soil offers a huge resistance to airflow and thus advective transport. Second, the increase in "advective potential" is inadequate to cause the same sort of effect as observed at the ASU house, and a preferential source of contaminant vapors is also required - two conditions that were seemingly fulfilled at the ASU house.

The removal of the gravel sub-base likewise also has a significant effect on the modeling results, and without it the full potential of a preferential pathway is seemingly unrealized. This can again be understood by understanding the significant resistance to contaminant transport that soils can present. This adds a third condition

for such a preferential pathways influence - a medium for effective communication between the preferential pathway and indoor environment is necessary.

This can be shown by analyzing the Péclet number for transport through the foundation crack. The Péclet number is a dimensionless number defined as the ratio between advective and diffusive transport across some characteristic length, i.e. it tell us if transport is advective or diffusion dominated. For transport through the foundation crack we define this as

$$\mathrm{Pe} = \frac{\text{advection}}{\text{diffusion}} = \frac{u_{\mathrm{ck}} L_{\mathrm{slab}}}{D_{\mathrm{g}}} \tag{1.1}$$

here $u_{\mathrm{ck}}$ $[\mathrm{m\,s^{-1}}]$ is the airflow velocity across through the crackl $L_{\mathrm{slab}} = 15\,\mathrm{cm}$ is the thickness of the foundation slab, i.e. the characteristic length; and $D_g = 6.87 \times 10^{-6}\,\mathrm{m^2\,s^{-1}}$ is the diffusivity of TCE in pure air.

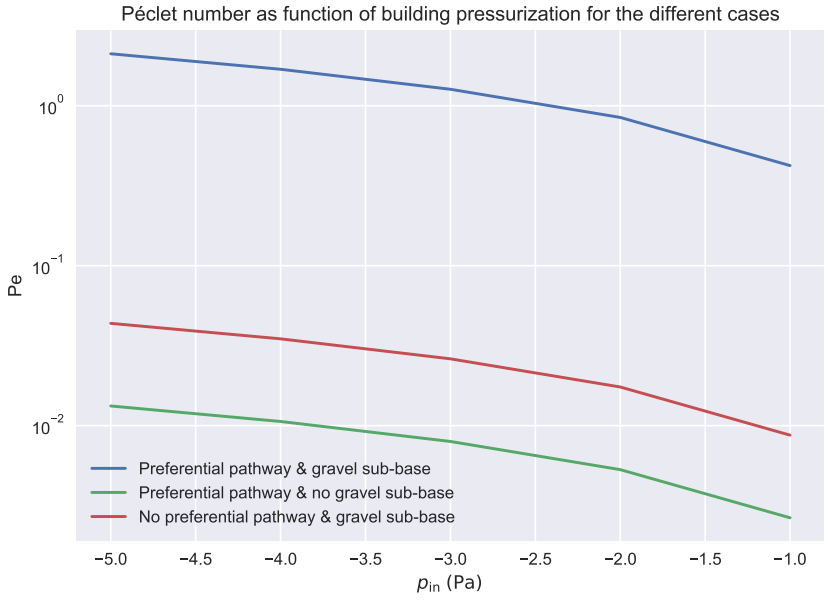


Figure 1.12: Péclet number for transport through the foundation crack of our modeled house as a fucntion of building pressurization. Here we consider three cases where the preferential pathway and gravel sub-base are present/absent, which shows the dramatic effect these site features can have on contaminant transport at a VI site.

The value of Pe charcterizes transport as such:

| | |
|---|---|
| $\mathrm{Pe} \gg 1$ | Advection dominated |
| $\mathrm{Pe} \ll 1$ | Diffusion dominated |
| $\mathrm{Pe} = 1$ | Advection and diffusion equal |

Figure 1.12 shows the Péclet number for three of the modeled cases:

1. Preferential pathway and gravel sub-base layer present
2. Preferential pathway present but gravel sub-base layer absent

3. Preferential pathway absent but gravel sub-base layer present

Note that the cases when $p_{\text{in}} > 0\,\text{Pa}$ are not plotted, as the only different is the sign of the Péclet number - by our definition $u_{\text{ck}} > 0$ indicates airflow into the house. This figure shows that it is only through the combination of a preferential pathway and a gravel sub-base layer that advective transport is able to dominate; diffusive transport dominates for the other cases which explains the weak correlation between $\alpha_{\text{gw}}$ and $p_{\text{in}}$ in Figure 1.11 when the preferential pathway was removed. Likewise it explains the dramatic increase of $\alpha_{\text{gw}}$ as $p_{\text{in}}$ decreases when the gravel sub-base and preferential pathway were present, as advective transport only starts to dominate after $p_{\text{in}} < -2.5\,\text{Pa}$.

To summarize, for a preferential pathway to have a significant influence at a VI site, the following conditions need to be fulfilled:

1. A preferential source of air in required to enhance the advective transport potential at the site.

2. Contaminant vapors must likewise be preferentially supplied.

3. There needs to exist a medium to facilitate effective communication between the preferential pathway and the indoor environment.

While this may seem like some specific conditions to be fulfilled for a preferential pathway to be so impactful, it can easily be generalized to other scenarios. For instance, one could easily imagine a situation where a house has a gravel backfill surrounding it, with some other subsurface source - like a leaky sewer pipe (that does not exit anywhere the building). Under such a circumstance, one could conceivably observe a similar effect in the indoor contaminant concentration caused by a very different scenario.

### 1.4.1 Role Of Air Exchange Rate

Simulations so far has assumed that air exchange rate is at a constant $0.5\,\text{h}^{-1}$ irrespective of the house pressurization. This is not quite realistic, as air exchange rates are constantly fluctuating, and this will have an impact on indoor contaminant concentrations. To account for this, we will again rerun our model simulations, but this time assuming different air exchange rate values, and if this can capture some more of the observed variability.

Ideally, we would wish to be able to determine air exchange rate based on site conditions, and in particular building pressurization. Determining air exchange rate exactly is difficult, and is influenced by building pressurization, indoor/outdoor temperature differences, wind, operation of HVAC systems, etc. This is a topic that will be expanded on in Chapter (TBD).

Air exchange rates are usually legally regulated as part of local building ordinances, and depending on the type of building, its values and bounds are usually more or less known. Instead, we will rerun the model and assume a wider range of constant air exchange rate values. At the ASU house, air exchange rates were measured using a tracer-gas study, and the the 10th, 50th, and 90th percentile air exchange rate values, as well as the corresponding values from the EPA duplex, and an independent EPA study that measured air exchange rates nationwide in the

USA, all of which can be seen in Table 1.1. Based on this we will rerun the model using air exchange values of 0.1, 0.5, and $0.9\,\mathrm{h}^{-1}$.

| | Percentile | | |
|---|---|---|---|
| | 10th | 50th | 90th |
| EPA study[17, 18] | 0.16-0.2 | 0.35-0.49 | 1.21-1.49 |
| ASU house[3, 10] | 0.21 | 0.43 | 0.78 |
| EPA duplex[7] | 0.34 | 0.74 | 1.27 |

Table 1.1: Air exchange rate values [$\mathrm{h}^{-1}$]

Figure 1.13 shows the result of incorporating a wider range of air exchange rates when predicting $\alpha_{\mathrm{gw}}$. Here the central lines are the result corresponding to $A_e = 0.5\,\mathrm{h}^{-1}$, while the upper and lower bounds of each shaded area correspond to $A_e = 0.1$ and $0.9\,\mathrm{h}^{-1}$ respectively. The shaded area cover much of the confidence interval of $\alpha_{\mathrm{gw}}$ as a function of $p_{\mathrm{in}}$ This indicates that much of the uncertainty of numerically determining $\alpha_{\mathrm{gw}}$ could be accounted for by considering the range of air exchange values at a site; a "numerical confidence interval" of sorts.

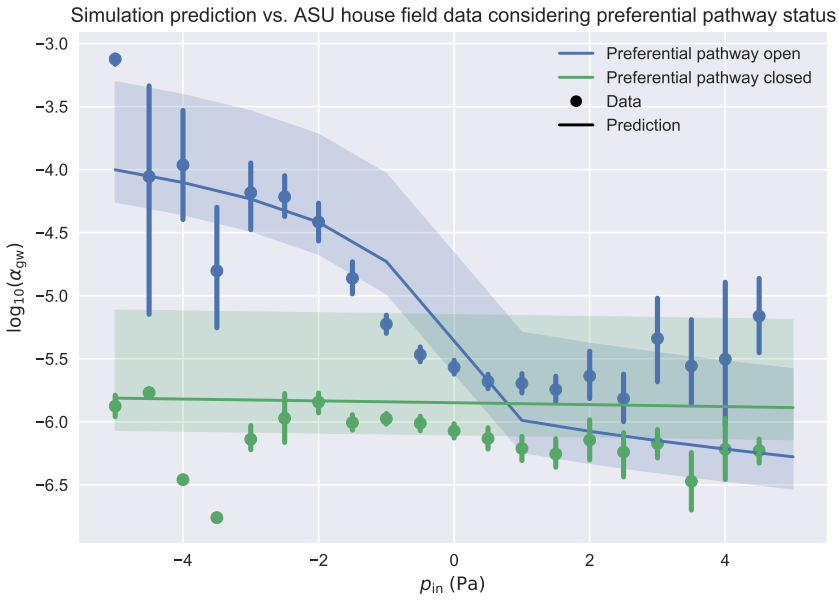


Figure 1.13: Modeling result from Figure 1.10 but with added shaded area to demonstrate the effect of different air exchange values. The central lines are the result corresponding to $A_e = 0.5\,\mathrm{h}^{-1}$, while the upper and lower bounds of each shaded area correspond to $A_e = 0.1$ and $0.9\,\mathrm{h}^{-1}$ respectively.

This concept of using pressure and air exchange rate is applied to a transient simulation, where we try to model a "typical" day by using the median diurnal variation of $p_{\mathrm{in}}$ and $A_e$ are used as model inputs, where we consider our model with and without the preferential pathway present. Specifically, we will use the median diurnal values of $p_{\mathrm{in}}$ and $A_e$ at one hour intervals over a 24-hour period from the ASU house and interpolating using cubic splines between these for continuity. This

will be put into contrast for a case where we only use the median diurnal values of $p_{\text{in}}$ but keep $A = 0.5\,\text{h}^{-1}$ constant.

Figure 1.14 shows how $\alpha_{\text{gw}}$ varies throughout this hypothetical "typical" day. Here we see that when the preferential pathway is present, variability of $\alpha_{\text{gw}}$ is mostly driven by fluctuations in contaminant entry rate; the variable and constant air exchange rate cases do not differ much from each other. When the preferential pathway is absent, then there is no variability of $\alpha_{\text{gw}}$ unless the air exchange rate is fluctuating.

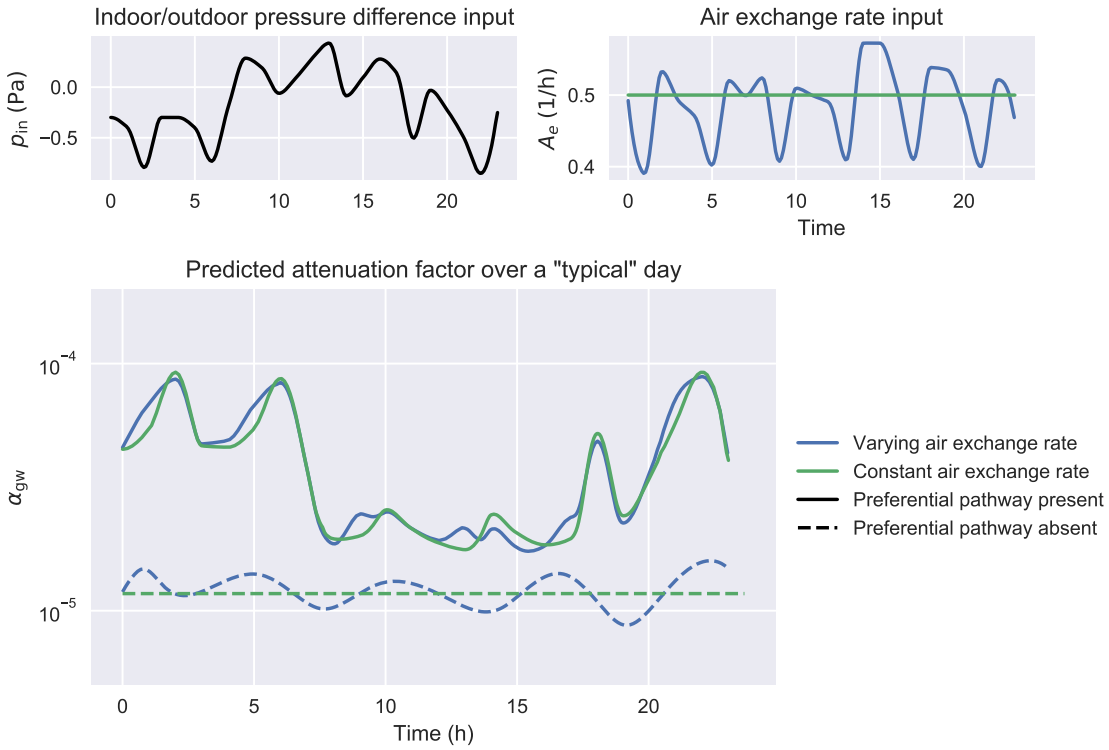


Figure 1.14: Modeled indoor contaminant concentration (as attenuation from groundwater) over a "typical" day. Here the hourly median indoor/outdoor pressure difference and air exchange rates recorded at the ASU house, as well as a comparison case where a constant air exchange rate of $0.5\,\text{h}^{-1}$ is assumed, are used as model input parameters. For these we consider two models cases; one where a preferential pathway is present and absent respectively.

To quantify the predicted variability of $\alpha_{\text{gw}}$ we define ratio between the minimum and maximum $\alpha_{\text{gw}}$ as

$$\Delta_{\text{max}} = \frac{\alpha_{\text{gw,max}}}{\alpha_{\text{gw,min}}} \tag{1.2}$$

Applying this to the cases where air exchange rate is varied, and the preferential pathway present/absent we find that these ratios are $\Delta_{\text{max}} = 5.09$ and $\Delta_{\text{max}} = 1.68$ respectively. I.e. $\alpha_{\text{gw}}$ may be expected to vary around half an order of magnitude at site characterized by a preferential pathway under our considered conditions, whereas one where there is no preferential pathway may vary by a factor of 1.68.

These "maximum daily variability" $\Delta_{\text{max}}$ values can be compared to those at the ASU house. Indoor contaminant concentration samples at the ASU house were collected roughly every four hours across the study period. By excluding the CPM

period, and then resampling these data on a daily basis, we can find $\Delta_{\max}$ for each day. These data are further separated to consider the period before and after the land drain preferential pathway was closed. The period before the preferential pathway was closed then includes 441 days or data points, giving a median value $\Delta_{\max} = 2.33$. For the period after the preferential pathway was closed, we get 181 days of data, giving a median value of $\Delta_{\max} = 1.60$. Thus, we can see that we somewhat overpredicted the expected variability for the period when the preferential pathway was open, but quite close when it was closed.

This indicates that for sites that are characterized by diffusive transport, much of the observed variability of indoor contaminant concentrations are driven by fluctuations in air exchange rate. For sites dominated by advective transport, fluctuations in building pressurization, and subsequently contaminant entry, are more important drivers are temporal variability of $\alpha_{\text{gw}}$.

## 1.5 Soil-Gas Spatial Variability And Preferential Pathways

Another aspect that preferential pathways has a significant impact on is spatial variability of contaminant vapors at a site. This can manifest inside the house itself, as large concentration differences between compartments, as was in the case of the leaky bathroom plumbing fixtures in the work by Pennell et al.[12]; here contaminant concentration were significantly higher in the upstairs bathroom than the basement, where higher concentrations are usually expected. These spatial variability can also manifest in the subsurface, which can be caused by a contaminant source[19], the building itself[20], or as we will explore here - a subsurface preferential pathways.

### 1.5.1 ASU House

Guo et al.[10] explored the role that the ASU house land drain preferential pathway had on the spatial variability of contaminant vapors in the subsurface, and in particular in the gravel sub-base. They used Kriging interpolation to visualize the distribution of subsurface contaminant vapors using their collected subsurface contaminant vapor samples. One snapshot of this work can be seen in Figure 1.15 where it clearly visible how the preferential pathway dramatically increased the contaminant vapor concentration in one half of the gravel sub-base layer - the half where the land drain preferential pathway exit was located.

While this undoubtedly demonstrates the influence of such a preferential pathway on spatial variability, it can be quantitively explored to show just how significant it can be. To do this, we consider the attenuation from the sub-slab region to the indoor environment

$$\alpha_{\text{subslab}} = \frac{c_{\text{in}}}{c_{\text{subslab},5}} \tag{1.3}$$

using sub-slab vapor contaminant concentration data from location 5 (see Figure **??**); this was the sample location closest to exit of the land drain preferential pathway. These data are visualized in a boxplot in Figure 1.16 where we considers the effects of CPM and the land drain preferential pathway on $\alpha_{\text{subslab}}$.

Here we that when the preferential pathway was open and the CPM system active, $\alpha_{\text{subslab}}$ usually exceeds unity by at least an order of magnitude, a situation

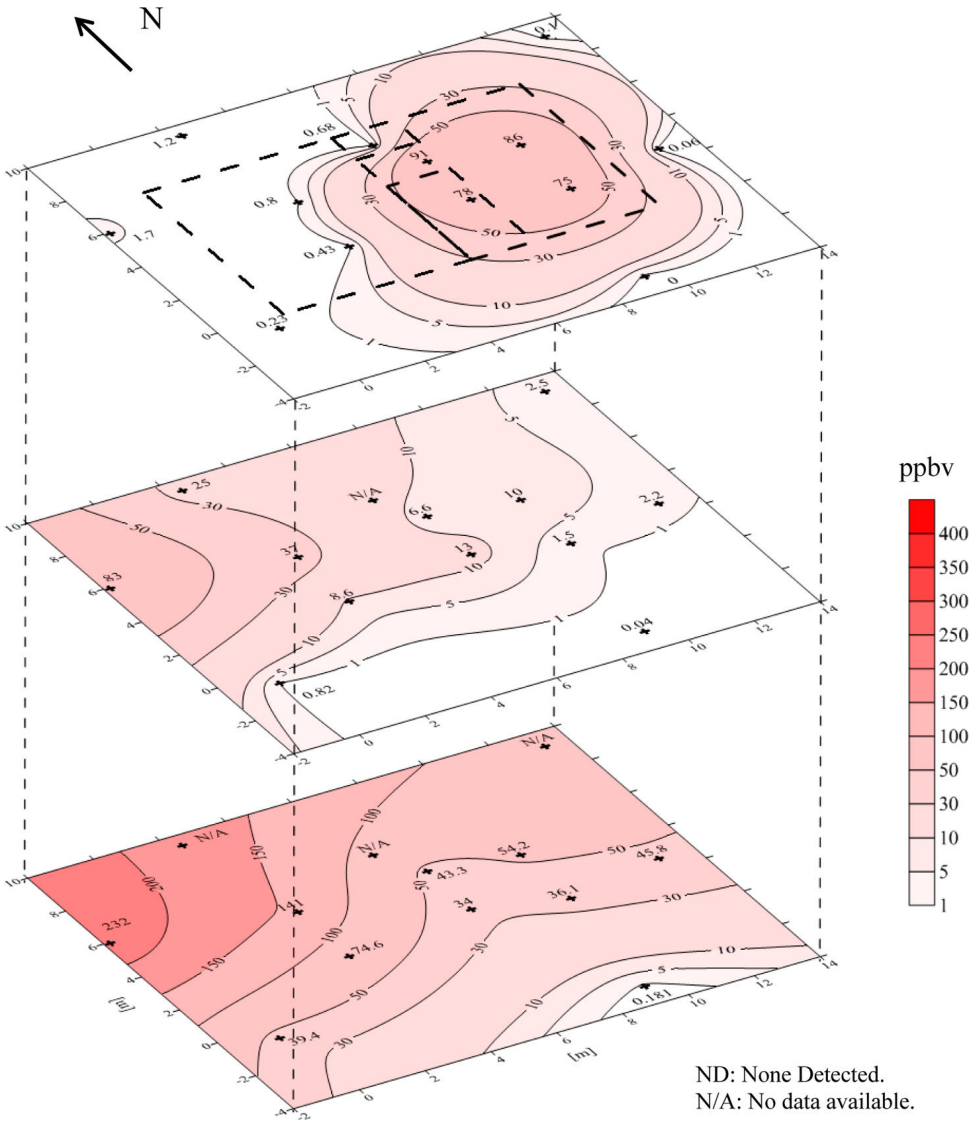


Figure 1.15: Distribution of TCE contaminant vapors in the subsurface underneath the ASU house. The top layer is right beneath the foundation, with the two subsequent at 0.9 m and 1.8 m below the foundation slab. Snapshot from the period when the CPM system was active. Figure from Guo et al.[10].

that should be impossible due to mass conservation; we can likewise see that this is an observed occurrence when the preferential pathway was open by CPM system inactive. Normally, one would not even expect $\alpha_{\text{subslab}}$ to be on the order of unity, and looking at the $\alpha_{\text{subslab}}$ data from the period after the preferential pathway was closed, as well as $\alpha_{\text{subslab}}$ data collected by the EPA in their VI database, $\alpha_{\text{subslab}}$ would be expected to range from $1 \times 10^{-3}$ to $1 \times 10^{-1}$ with $3 \times 10^{-2}$ a commonly recognized value[1]. Obviously, this is not a violation of mass conservation, but simply an indicator that even though location 5 is only 2 m away from the land drain preferential pathway exit, samples taken here clearly fail to capture the highest sub-slab contaminant concentrations; the highest contaminant vapor concentration in the subslab during the preferential pathway open period could have been order of magnitude higher than recorded.

This highlights the large impact that a preferential pathway can have on sub-

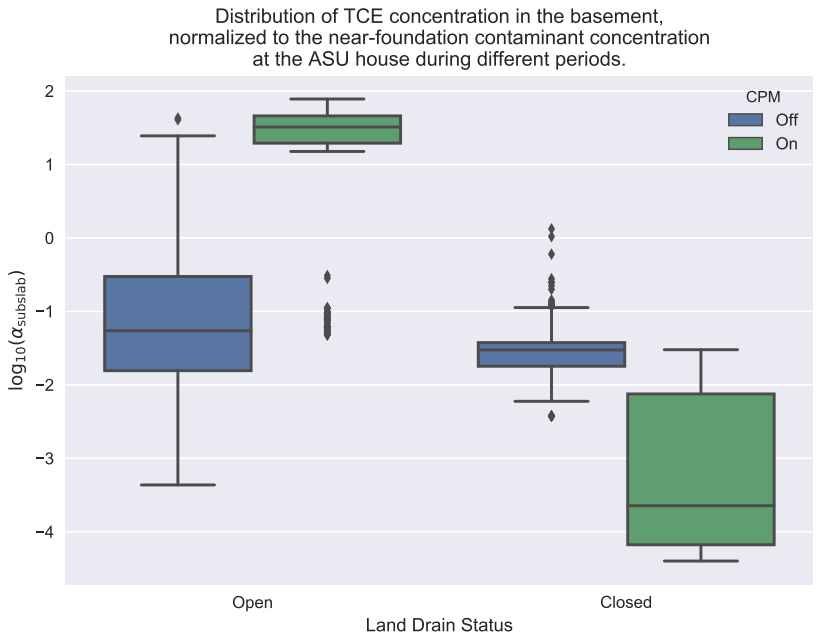


Figure 1.16: Boxplot showing the distribution of $\alpha_{\text{subslab}}$ considering the effects of CPM and the ASU house land drain preferential pathway. Here $\alpha_{\text{subslab}}$ is the attenuation from sub-slab sampling location 5 to the indoor environment. The box signifies the interquartile range (IQR) of values, with the central line representing the median value, and the top and bottom of the box are the 25th and 75th percentiles. The whiskers extend to 1.5 times the IQR. Markers indicate outlier data points that fall outside the whiskers.

surface spatial contaminant concentration variability. However, one conclusion from such high $\alpha_{\text{subslab}}$ values is that they may indicate that there are some indoor contaminant sources present - which was not the situation at the ASU house. Therefore, this is another aspect of VI that investigators should be cognizant abo ut; very large $\alpha_{\text{subslab}}$ values could be an indicate an indoor source *or* the existence of some preferential pathway at the VI site.

### 1.5.2 EPA Duplex

*This is purposely left empty for now.*

# Bibliography


[1] U.S. Environmental Protection Agency. *OSWER Technical Guide for Assessing and Mitigating the Vapor Intrusion Pathway From Subsurface Vapor Sources To Indoor Air*. 2015.

[2] David Folkes et al. "Observed Spatial and Temporal Distributions of CVOCs at Colorado and New York Vapor Intrusion Sites". en. In: *Ground Water Monit. Remediat.* 29.1 (Jan. 2009), pp. 70–80. ISSN: 1745-6592. DOI: 10/fw6kxz.

[3] Chase Holton et al. "Temporal Variability of Indoor Air Concentrations under Natural Conditions in a House Overlying a Dilute Chlorinated Solvent Groundwater Plume". In: *Environ. Sci. Technol.* 47.23 (Dec. 2013), pp. 13347–13354. ISSN: 0013-936X. DOI: 10/gd6dfd.

[4] Jill E. Johnston and Jacqueline MacDonald Gibson. "Spatiotemporal Variability of Tetrachloroethylene in Residential Indoor Air Due to Vapor Intrusion: A Longitudinal, Community-Based Study". En. In: *J. Expo. Sci. Environ. Epidemiol.* 24.6 (Nov. 2014), p. 564. ISSN: 1559-064X. DOI: 10/f6m5wc.

[5] Vitthal Hosangadi et al. "High-Frequency Continuous Monitoring to Track Vapor Intrusion Resulting From Naturally Occurring Pressure Dynamics". en. In: *Remediation* 27.2 (Mar. 2017), pp. 9–25. ISSN: 1520-6831. DOI: 10/gd6df5.

[6] Thomas McHugh, Per Loll, and Bart Eklund. "Recent Advances in Vapor Intrusion Site Investigations". In: *Journal of Environmental Management*. Global Trends in the Environmental Remediation Industry 204 (Dec. 2017), pp. 783–792. ISSN: 0301-4797. DOI: 10/gd6dgk.

[7] U.S. Environmental Protection Agency. *Assessment of Mitigation Systems on Vapor Intrusion: Temporal Trends, Attenuation Factors, and Contaminant Migration Routes under Mitigated And Non-Mitigated Conditions*. en. 2015.

[8] Lynn Marie Hubbard and Nils Hagberg. "Time-Variation of the Soil Gas Radon Concentration under and near a Swedish House". In: *Environment International*. The Natural Radiation Environment VI 22 (Jan. 1996), pp. 477–482. ISSN: 0160-4120. DOI: 10.1016/S0160-4120(96)00148-1.

[9] Paul C. Johnson et al. *Integrated Field-Scale, Lab-Scale, and Modeling Studies for Improving Our Ability to Assess the Groundwater to Indoor Air Pathway at Chlorinated Solvent-Impacted Groundwater Sites*. en. 2016.

[10] Yuanming Guo et al. "Identification of Alternative Vapor Intrusion Pathways Using Controlled Pressure Testing, Soil Gas Monitoring, and Screening Model Calculations". In: *Environ. Sci. Technol.* 49.22 (Nov. 2015), pp. 13472–13482. ISSN: 0013-936X. DOI: 10/f72b6n.

[11] Thomas McHugh et al. “Evidence of a Sewer Vapor Transport Pathway at the USEPA Vapor Intrusion Research Duplex”. In: *Science of The Total Environment* 598 (Nov. 2017), pp. 772–779. ISSN: 0048-9697. DOI: 10/gd6dfz.

[12] Kelly G. Pennell et al. “Sewer Gas: An Indoor Air Source of PCE to Consider During Vapor Intrusion Investigations”. en. In: *Groundwater Monit R* 33.3 (Aug. 2013), pp. 119–126. ISSN: 1745-6592. DOI: 10/gd6dd9.

[13] Karin Birn Nielsen and Boerge Hvidberg. “Remediation Techniques for Mitigating Vapor Intrusion from Sewer Systems to Indoor Air”. en. In: *Remediat. J.* 27.3 (June 2017), pp. 67–73. ISSN: 1520-6831. DOI: 10/gd6ddz.

[14] Chase Holton et al. “Long-Term Evaluation of the Controlled Pressure Method for Assessment of the Vapor Intrusion Pathway”. In: *Environ. Sci. Technol.* 49.4 (Feb. 2015), pp. 2091–2098. ISSN: 0013-936X. DOI: 10/f64j45.

[15] *Indianapolis Research Duplex Total Database - Data.Gov*. https://catalog.data.gov/dataset/research-duplex-total-database.

[16] Yuanming Guo. “Vapor Intrusion at a Site with an Alternative Pathway and a Fluctuating Groundwater Table”. PhD Thesis. Arizona State University, 2015.

[17] U.S. EPA. *Exposure Factors Handbook 2011 Edition*. en. Tech. rep. U.S. Environmental Protection Agency, 2011, p. 1436.

[18] M. D. Koontz and H. E. Rector. *Estimation of Distributions for Residential Air Exchange Rates*. Tech. rep. U.S. Environmental Protection Agency, Mar. 1995.

[19] Judith Chow et al. “Concentration of Tetrachloroethylene in Indoor Air at a Former Dry Cleaner Facility as a Function of Subsurface Contamination: A Case Study”. In: *J. Air Waste Manag. Assoc.* 57.6 (June 2007), pp. 753–760. ISSN: 1047-3289. DOI: 10/c6n8x9.

[20] Chase Holton et al. “Creation of a Sub-Slab Soil Gas Cloud by an Indoor Air Source and Its Dissipation Following Source Removal”. en. In: *Environ. Sci. Technol.* 52.18 (Aug. 2018), pp. 10637–10646. ISSN: 0013-936X, 1520-5851. DOI: 10/gd569z.